RSC Advances

COMMUNICATION

View Article Online
View Journal | View Issue

Cite this: *RSC Adv.*, 2015, **5**, 9861

Received 3rd November 2014
Accepted 6th January 2015

DOI: 10.1039/c4ra13705a

www.rsc.org/advances

TiO_2 nanosheet array thin film for self-cleaning coating

Furong Wang,[ab] Guoqiang Zhang,[ab] Zhao Zhao,[ab] Huaqiao Tan,[a] Weixing Yu,[c] Xuming Zhang[d] and Zaicheng Sun*[a]

A simple hydrothermal method is developed to directly grow TiO_2 nanosheets on a bare glass substrate. By tuning the reaction conditions, the thickness of the TiO_2 nanosheet layer can be tuned from tens to hundreds of nanometers. This TiO_2 nanosheet layer exhibits good transparency due to the air pocket existing inside the thin film layer between nanosheets. On the other hand, the TiO_2 layer has a good hydrophilic surface and good wettability, especially under UV light illumination. The degradation of dye (rhodamine B) results indicate that the TiO_2 nanosheet coating has excellent photocatalytic activity. All these results demonstrate that the TiO_2 nanosheet coating could be a highly transparent self-cleaning coating.

Introduction

A coating with self-cleaning properties would be interesting and attractive since it could save a lot of time and cost for maintenance of building and solar panels.[1] Self-cleaning coatings are primarily categorized into hydrophobic and hydrophilic,[2–7] and both these types clean the surfaces by their different behavior towards water. The former makes the water droplets slide and roll over the surfaces, thereby carrying the dirt away with them to mimic a natural lotus leaf. Much effort has been devoted to try to mimic the self-cleaning property of the lotus leaf.[8,9] The latter uses appropriate metal oxides with hydrophilic surface to sheet the water that removes the dirt from the surface.[7,10] In addition to the sheeting effect, metal oxides have an additional property of chemically breaking down organic dirt deposits by a sunlight-assisted cleaning mechanism, *i.e.* photocatalytic effect of TiO_2. Among all kinds of metal oxides, TiO_2 has been one of the most investigated engineering materials during recent decades, especially in the arena of energy and environmental applications, due to its advantage of good photocatalytic activity and photostability and low cost.[11–13] The photocatalytic property of TiO_2 relies on the access of high energy facets such as (001) and surface area. Making TiO_2 coating with large surface area and high-energy facet will enhance its photocatalytic activity.[14]

TiO_2-based coatings can be applied easily on transparent substrates such as glass and plastics to provide a self-cleaning function. However, the coatings developed thus far always enhance the surface reflection of transparent substrates due to the large refractive index of TiO_2 ($n \approx 2.52$–2.76). Reflection at the air–glass interface is about 4% for normal incident light; whereas at the air–TiO_2 interface reflection for normal incident light could be as high as 20%.[15] For some applications, such as solar cells, windows, a high transmittance for visible light is desirable.[14,16] Developing nanostructural TiO_2 coating is an effective route to lower the refractive index of TiO_2 layer and reflectivity of interface. Fujishima and coworkers reported the TiO_2/SiO_2 multiple layers for the self-cleaning coating with antireflective properties.[14,15] Recently our group developed TiO_2 and ZnO@TiO_2 nanowire array for the self-cleaning coating, exhibiting good photocatalytic performance and stability.[10,17] However, FTO was often employed as a substrate for the nanowires array growing in both cases. Herein, we further develop TiO_2 nanosheets array directly grown on the bare glass. By tuning the reaction conditions, the thickness and density of TiO_2 nanosheets can be finely adjusted. This TiO_2 nanostructure enhance the transmittance of glass accompanying with excellent photocatalytic properties due to porous TiO_2 nanosheet exposed with (001) facet structures. The wettability of the TiO_2 nanosheet array was characterized by contact angle measurement. Although the contact angle increases with the increasing of density of TiO_2 nanosheet, it clearly decreases after illuminate with UV light irradiation. That indicates that the TiO_2 nanosheet layer has a good hydrophilic property. This

[a]*State Key Laboratory of Luminescence and Applications, Chagchun Institute of Optics, Fine Mechanics and Physics, 3888 East Nanhu Road, Changchun, Jilin 130033, P. R. China. E-mail: sunzc@ciomp.ac.cn*

[b]*University of Chinese Academy of Sciences, Beijing, P. R. China*

[c]*Insititue of Micro and Nano Optics, College of Optoelectronic Engineering, Shenzhen University, Shenzhen 518060, P. R. China. E-mail: yuwx@szu.edu.cn*

[d]*Department of Applied Physics, The Hong Kong Polytechnic University, Hong Kong SAR, China*

route shows great potential for self-cleaning application in the solar cells and windows.

Experimental

Chemicals and materials

Isopropanol (AR grade) was purchased from the Tianjin Fuyu fine Chemical Co. Ltd. Ethanol (AR grade) and hydrochloric acid (AR grade) were purchased from the Beijing Chemical factory. Tetrabutyl orthotitanate (AR grade) was purchased from the Tianjin Guangfu Chemical Reagent Co. Ltd. And other reagents, Titanium(IV) isopropoxide (TIP, AR grade), diethylenetriamine (DETA, AR grade) and rhodamine B (Rh B, AR grade), are purchased from the Aladdin Reagent Company. All of the materials in these experiments were used without further purification.

Synthesis of TiO_2 nanosheet thin film

Firstly, we dip-coated a layer of dense TiO_2 from TiO_2 sol–gel precursor on the bare glass substrates (25 × 25 mm^2), which were ultrasonically cleaned with deionized water, ethanol, acetone and isopropanol, at speed of 20 mm min^{-1}. TiO_2 sol–gel precursor was prepared by stirring the mixture of 30 mL isopropanol, 1.2 mL hydrochloric acid and 2.04 g tetrabutyl orthotitanate over 30 minutes. The amorphous TiO_2 was transferred into TiO_2 nanocrystal seeds layer by thermal-treating the pre-coated glass in an electric oven at 450 °C for 4 h. Next, after 15 min plasma surface treatment, the glass with TiO_2 seed layer was placed into a Teflon lined stainless steel autoclave, which contained 30 μL DETA, 30 mL isopropanol and a variable amount (200–400 μL in this study) of TIP. The sealed autoclave was heated to 180 °C for 18 h in an electric oven. Then, the reaction was naturally cooled to room temperature. The as-prepared samples were gently rinsed with ethanol and dried at room temperature. Finally, the samples were annealed at 400 °C for 1 h to form the crystal.

Characterization

The morphology of the samples was measured with a JEOL JSM 4800F field emission scanning electron microscope (FE-SEM). Transmission electron microscopy (TEM) images were taken from a FEI Tecnai G2 transmission electron microscopy. X-ray diffraction patterns were obtained on Bruker AXS D8 Focus Diffractometer using Cu Kα radiation ($\lambda = 1.54056$ Å). The UV-Vis transmittance spectra were carried out by a Shimadzu UV-3600 UV-Vis scanning spectrophotometer. The contact angle (CA) were measured by a KRUSS GH-100 universal surface tester, and the CA photos were recorded by a CCD camera interfaced with an optical microscope, which was arranged in a goniometric setup.

Rhodamine B (Rh B) photo-degradation activity measurements

Rh B ethanol solution of 5000 ppm was prepared for dye degradation in the experiment. Three selected samples (marked as TIP-200, TIP-300, TIP-400 prepared from 200, 300 and 400 μL TIP as Ti source, respectively) were compared for photocatalytic reaction. All samples were dipped in Rh B ethanol solution and kept out of the light for 24 hours. Then the samples were removed and dried naturally so that a layer of Rh B formed on the sample surface. The photocatalytic activity of the samples was evaluated by monitoring the decolorization of rhodamine B (Rh B) irradiated by a 300 W UV-light xenon lamp (AM1.5) at 15 cm distance. The samples without any previous treatment were covered with Al foil from any other light source before irradiation. When irradiated for the specified time, the maximum peak (553 nm) of absorbance band was monitored by a Shimadzu UV-3600 UV-Vis spectrophotometer to estimate the amount of Rh B.

Results and discussion

Recently, Lou *et al.* developed a simple hydrothermal route to synthesize TiO_2 spheres composed of nanosheets with exposed highly reactive (001) facets, which possessed high surface area and good photocatalytic activity.[18] We have demonstrated the TiO_2 nanosheets can grow on the ZnO nanowire surface.[19] This provides an opportunity to fabricate TiO_2 nanostructure on the substrate like glass, FTO and ITO and so on. In this report, we developed TiO_2 nanosheets array grown on the glass through modified Lou's route. As shown in the Fig. 1, a layer of TiO_2 seed was firstly applied on the bare glass substrate to obtain uniformly and fully covered TiO_2 nanosheet array. TiO_2 nanosheets array was then grown in the TIP and DETA solution at 180 °C for 18 hours. The plan and cross-section view of as-grown TiO_2 nanosheets arrays were displayed in the Fig. 2. From the top view FE-SEM images, the TiO_2 nanosheets density increases with the initial TIP amount. Some TiO_2 spheres will attach on the surface of substrate when TIP amount is too high. That may lead to scattering and loses the transmittance of glass. From the cross-section FE-SEM images (Fig. 2D–F), the thicknesses of the TiO_2 nanosheets array are 80, 130, 150 nm for the TIP-200, 300 and 400, respectively. It should be noted that the thickness contain the ~30 nm of TiO_2 seed layer. We also investigate the effect of reaction time on the TiO_2 layer. The TiO_2 nanosheets can not fully cover the substrate when the reaction time is less than 8 hours and the thickness has slightly different for the 12 to 18 hours when other reaction conditions keep same as TIP-300.

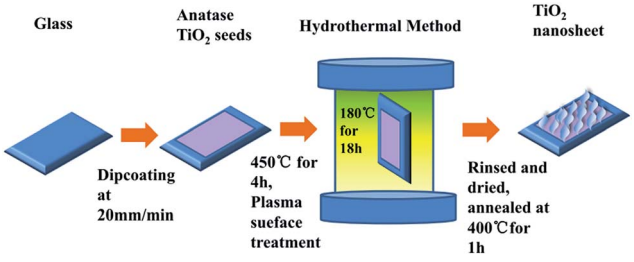

Fig. 1 Schematic diagram of the preparation procedure for the TiO_2 nanosheets array on the bare glass substrate through hydrothermal route.

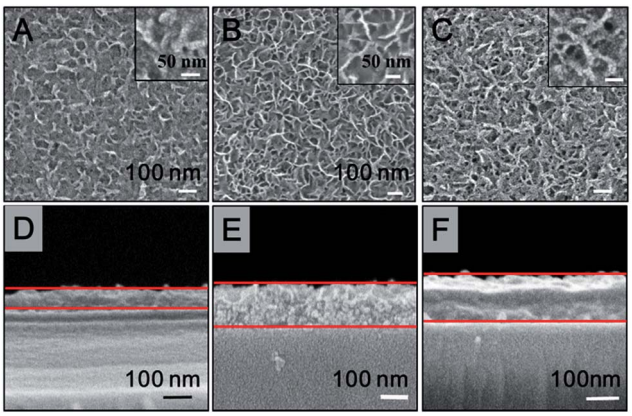

Fig. 2 FE-SEM images (plan view A–C and cross-sectional view D–F) of TiO_2 nanosheets array thin film prepared from TIP-200 (A and D), TIP-300 (B and E) and TIP-400 (C and F) in 30 mL isopropanol with 30 μL DETA, respectively. The insets in (A–C) are high magnification images for (A–C).

As we know, anatase TiO_2 has the best photocatalytic activity among the three crystalline phase-anatase, brookite and rutile. In order to transfer the TiO_2 nanosheets into anatase phase, the samples were calcined at 400 °C for 1 hour. X-ray diffraction (XRD) pattern, as shown in Fig. 3A, shows the diffraction peaks at 25.3, 37.8, 48.0 corresponding to anatase TiO_2 (JCPDS no. 21-1272) (101), (004) and (200), respectively. Furthermore, we can confirm the crystalline TiO_2 from transmission electron microscopy (TEM) images. Fig. 3B shows that the TiO_2 thin film contains thin petal-like TiO_2 nanosheet structures. High resolution TEM images exhibit that the nanosheet structures have clear crystalline lattice structures. It can be observed that there is a set of lattices with an equal interfringe spacing of 0.24 and 0.19 nm, corresponding to the anatase (020) and (200) planes. According to previous reports,[17,20] the TiO_2 nanosheets are bound by (001) facets on both of the exposed sides.

Due to TiO_2 has large refractive index (n = 2.5–2.7), ~20% reflectivity at air-TiO_2 interface make the transmittance of glass loss too much. For the windows and solar cells applications, high transparency is highly desired. Fig. 4A shows the transmittance of the bare glass substrate coated with the TiO_2 nanosheets thin films of different thickness. The bare glass shows ~90% transmission. The TIP-200 shows low transparency (~60%), which is close to the glass coated with dense TiO_2 thin film. The TIP-200 shows looser nanosheet structures and thinner coating thickness. That is the reason why TIP-200 displays low transparency. When the thickness of TiO_2 nanosheets array increases to 150 nm, the transmittance of TIP-300 is close to that of bare glass. The main reason is that the dense TiO_2 nanosheets structure possesses huge amount air pocket in the thin film, which effectively decreases the refractive index of the whole coating layer. The maximum transmittance is 94.6% at 531 nm, which is better than the bare glass. When the TiO_2 nanosheets array further increases to 180 nm, the transmittance of TIP-400 decreases to 80%. From FE-SEM top image, the density of TIP-400 is the densest among the three samples, which has less air pocket. That results in TIP-400 has higher refractive index than that of TIP-300.

The wettability is another important factor for hydrophilic type self-cleaning coatings. Normally, the nanostructure may induce hydrophobic due to the fine air pocket.[21] Fig. 4B shows the contact angle of TIP-200, 300 and 400. It clearly shows the contact angle increase from 8.69°, 15.76° to 56.64° for TIP-200, 300 and 400, respectively. After UV light illumination, the contact angle can be severally decreased to 5.79°, 8.20° and 31.27°. These results indicate the TIP-300 coating has good hydrophilic property for self-cleaning coating.

The photocatalytic activity of the coating layer is a key issue for hydrophilic self-cleaning coatings. Rhodamine B (Rh B), as a common dye mole, is often chosen as a model molecule for the study of organic molecules degradation. It is also suspected to be carcinogenic compound need be removed from drinking water. We chose Rh B as a model dye molecule to demonstrate the photocatalytic activity of the TiO_2 nanosheet thin films in this report. Fig. 5A shows the degradation of Rh B on the TiO_2 nanosheet thin films with different quantities of TIP. We can see the three curves are at similar degradation rate. And it's a little slow for TIP-200. After 35 minutes illumination under UV-Vis light, about 98% Rh B was degraded by the TiO_2 nanosheet thin films. The substrate turned from dark purple to transparent under the light illumination. Fig. 5B shows the durability

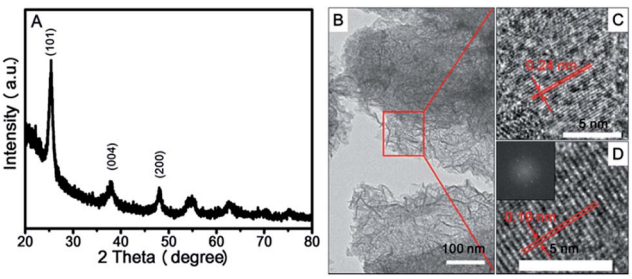

Fig. 3 Electron microscopy and XRD characterization of anatase TiO_2 nanosheet synthesized from 300 μL of TIP and 30 μL of DETA in 30 mL isopropanol at 180 °C for 18 hours. (A) XRD patterns of anatase TiO_2 nanosheet on glass. (B) Transmission electron microscopy (TEM) graphs of porous anatase TiO_2 nanosheets. The insets are high resolution TEM images of the selected area. (C and D) High resolution TEM image of the red square shown in (A). The top inset in (D) shows a fast Fourier transform micro-graph of the image area in (D).

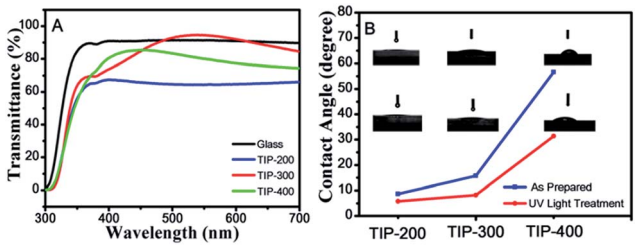

Fig. 4 (A) The transparency of the glass substrate and thin films of TiO_2 seeds with different thicknesses of TiO_2 nanosheets. (B) The contact angle of the TiO_2 nanosheet thin films coated with different thicknesses. The insets show the contact angle optical images.

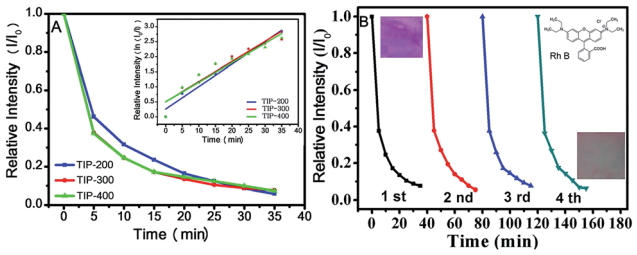

Fig. 5 (A) Comparison of the photocatalytic degradation rates of rhodamine B (Rh B) of the selected samples. Inset: ln-plot of the degradation rates of the TiO_2 nanosheet thin film with different thicknesses (B) cycling degradation curves of the TiO_2 nanosheet thin film (TIP-300) sample with optical pictures of the initial and final state in the cycle. The inset at right-up corner is the chemical structure of Rh B.

of the TiO_2 nanosheet thin films for the photocatalytic degradation of Rh B under UV-Vis irradiation. After each recycle experiment, the photocatalytic activity remains unchanged. These results indicate that the TiO_2 nanowires array exhibit good photocatalytic performance and durability.

Conclusions

In summary, we developed a simple synthesis route to fabricate the TiO_2 nanosheet array on the glass substrate. After 400 °C calcination, TiO_2 nanosheets are in anatase crystalline phase exposed with high-energy (001) facet. TiO_2 nanosheet array coating exhibits good transmittance due to the introduction of air pocket in the TiO_2 thin film. The contact angle obviously decreases after irradiation of UV-Vis light, indicating that the wettability of TiO_2 nanosheet array coating is improved. The degradation of Rh B indicates that TiO_2 nanosheet array has excellent photocatalytic performance. All these results imply that TiO_2 nanosheet array could be a high performance self-cleaning coating. The conclusions section should come at the end of article, before the acknowledgements.

Acknowledgements

The authors thank the National Natural Science Foundation of China (no. 21301166, 21201159, and 61361166004), Science and Technology Department of Jilin Province (no. 20130522127JH, and 20121801) are gratefully acknowledged. Z. S. thanks the support of the "Hundred Talent Program" of CAS. Supported by open research fund program of State Key Laboratory of Luminescence and Applications (CIOMP, CAS).

Notes and references

1 R. Blossey, *Nat. Mater.*, 2003, **2**, 301–306.
2 I. P. Parkin and R. G. Palgrave, *J. Mater. Chem.*, 2005, **15**, 1689–1695.
3 V. A. Ganesh, H. K. Raut, A. S. Nair and S. Ramakrishna, *J. Mater. Chem.*, 2011, **21**, 16304–16322.
4 V. A. Ganesh, A. S. Nair, H. K. Raut, T. M. Walsh and S. Ramakrishna, *RSC Adv.*, 2012, **2**, 2067–2072.
5 L. Peruchon, E. Puzenat, J. M. Herrmann and C. Guillard, *Photochem. Photobiol. Sci.*, 2009, **8**, 1040–1046.
6 Y. Lai, Y. Tang, J. Gong, D. Gong, L. Chi, C. Lin and Z. Chen, *J. Mater. Chem.*, 2012, **22**, 7420–7426.
7 L. W. Zhang, R. Dillert, D. Bahnemann and M. Vormoor, *Energy Environ. Sci.*, 2012, **5**, 7491–7507.
8 L. Feng, S. H. Li, Y. S. Li, H. J. Li, L. J. Zhang, J. Zhai, Y. L. Song, B. Q. Liu, L. Jiang and D. B. Zhu, *Adv. Mater.*, 2002, **14**, 1857–1860.
9 Z.-Z. Gu, H. Uetsuka, K. Takahashi, R. Nakajima, H. Onishi, A. Fujishima and O. Sato, *Angew. Chem., Int. Ed.*, 2003, **42**, 894–897.
10 P. Ragesh, V. A. Ganesh, S. V. Naira and A. S. Nair, *J. Mater. Chem. A*, 2014, **2**, 14773–14797.
11 M. R. Hoffmann, S. T. Martin, W. Y. Choi and D. W. Bahnemann, *Chem. Rev.*, 1995, **95**, 69–96.
12 T. L. Thompson and J. T. Yates, *Chem. Rev.*, 2006, **106**, 4428–4453.
13 W. Jiang, J. A. Joens, D. D. Dionysiou and K. E. O'Shea, *J. Photochem. Photobiol., A*, 2013, **262**, 7–13.
14 H. G. Yang, C. H. Sun, S. Z. Qiao, J. Zou, G. Liu, S. C. Smith, H. M. Cheng and G. Q. Lu, *Nature*, 2008, **453**, 638–641.
15 X. T. Zhang, O. Sato, M. Taguchi, Y. Einaga, T. Murakami and A. Fujishima, *Chem. Mater.*, 2005, **17**, 696–700.
16 P. Nostell, A. Roos and B. Karlsson, *Thin Solid Films*, 1999, **351**, 170–175.
17 J. S. Chen, Y. L. Tan, C. M. Li, Y. L. Cheah, D. Luan, S. Madhavi, F. Y. C. Boey, L. A. Archer and X. W. Lou, *J. Am. Chem. Soc.*, 2010, **132**, 6124–6130.
18 J. S. Chen, J. Liu, S. Z. Qiao, R. Xu and X. W. Lou, *Chem. Commun.*, 2011, **47**, 10443–10445.
19 R. Wang, H. Tan, Z. Zhao, G. Zhang, L. Song, W. Dong and Z. Sun, *J. Mater. Chem. A*, 2014, **2**, 7313–7318.
20 Z. Zhao, H. Tan, H. Zhao, D. Li, M. Zheng, P. Du, G. Zhang, D. Qu, Z. Sun and H. Fan, *Chem. Commun.*, 2013, **49**, 8958–8960.
21 M. H. Jin, X. J. Feng, L. Feng, T. L. Sun, J. Zhai, T. J. Li and L. Jiang, *Adv. Mater.*, 2005, **17**, 1977–1981.